

See discussions, stats, and author profiles for this publication at: <https://www.researchgate.net/publication/303866012>

Comparative study of thermodynamic properties near the structural phase transitions in $\text{Sr}_3\text{Rh}_4\text{Sn}_{13}$ and $\text{Sr}_3\text{Ir}_4\text{Sn}_{13}$

Article · June 2016

DOI: 10.1103/PhysRevB.93.245119

CITATIONS

4

READS

103

7 authors, including:



C. S. Lue

National Cheng Kung University

135 PUBLICATIONS 1,488 CITATIONS

SEE PROFILE



C. N. Kuo

National Cheng Kung University, Tainan

26 PUBLICATIONS 102 CITATIONS

SEE PROFILE



Yung-Kang Kuo

National Dong Hwa University

172 PUBLICATIONS 1,610 CITATIONS

SEE PROFILE

Some of the authors of this publication are also working on these related projects:



Ru₂NbGa: A Heusler-type compound with semimetallic characteristics [View project](#)

Comparative study of thermodynamic properties near the structural phase transitions in $\text{Sr}_3\text{Rh}_4\text{Sn}_{13}$ and $\text{Sr}_3\text{Ir}_4\text{Sn}_{13}$

C. S. Lue,^{1,*} C. N. Kuo,¹ C. W. Tseng,¹ K. K. Wu,² Y.-H. Liang,³ C.-H. Du,³ and Y. K. Kuo^{2,†}

¹*Department of Physics, National Cheng Kung University, Tainan 70101, Taiwan*

²*Department of Physics, National Dong Hwa University, Hualien 97401, Taiwan*

³*Department of Physics, Tamkang University, Tamsui 25137, Taiwan*

(Received 8 March 2016; revised manuscript received 3 May 2016; published 8 June 2016)

Structural phase transitions in $\text{Sr}_3\text{Rh}_4\text{Sn}_{13}$ and $\text{Sr}_3\text{Ir}_4\text{Sn}_{13}$ are currently of interest due to the evidence of strong correlation with their superconductivity. To further obtain additional insight into the thermodynamic properties of the phase transitions, we have performed a study of single-crystalline $\text{Sr}_3\text{Rh}_4\text{Sn}_{13}$ and $\text{Sr}_3\text{Ir}_4\text{Sn}_{13}$ by means of the specific-heat and thermal-expansion measurements, mainly focusing on the features around the phase-transition temperature $T^* \simeq 138$ and 147 K, respectively. In particular, the specific-heat data have been analyzed in the framework of the critical fluctuation model in addition to a mean-field contribution. Relatively large critical exponents were obtained for $\text{Sr}_3\text{Ir}_4\text{Sn}_{13}$, suggesting a shorter coherence length associated with the phase transition. For each compound, an enhancement in the mean-field jump compared to the BCS value has been quantitatively identified, revealing the strong-coupling characteristics for the observed phase transitions. Furthermore, prominent changes in the coefficient of linear thermal expansion and bulk modulus across T^* have been identified, providing new information about the structural phase transitions in the title compounds.

DOI: [10.1103/PhysRevB.93.245119](https://doi.org/10.1103/PhysRevB.93.245119)

I. INTRODUCTION

Recently, the phase transitions that take place at the transition temperature $T^* \simeq 138$ K in $\text{Sr}_3\text{Rh}_4\text{Sn}_{13}$ and $\simeq 147$ K in $\text{Sr}_3\text{Ir}_4\text{Sn}_{13}$ have attracted considerable attention due to the indications of strong interplay with their superconductivity occurring at much lower temperatures [1–9]. Single-crystal x-ray diffraction (XRD) analysis for both materials has revealed the presence of a structural phase transition at the corresponding T^* . The structural phase transition has been identified as a lattice distortion from a high-temperature cubic $\text{Yb}_3\text{Rh}_4\text{Sn}_{13}$ -type structure (space group $Pm\bar{3}n$) to a low-temperature phase with a lower crystallographic symmetry [1,4]. Further studies confirmed that the phase transition at T^* is associated with a substantial reduction in the Fermi-level density of states (DOS) but has no involvement in any magnetic ordering [1,2,4,6–9]. It has thus been speculated that the lattice distortions in $\text{Sr}_3\text{Rh}_4\text{Sn}_{13}$ and $\text{Sr}_3\text{Ir}_4\text{Sn}_{13}$ could arise from the charge-density-wave (CDW) instability [1,2,4–7]. Moreover, a systematic suppression in T^* along with an enhancement in the superconducting transition temperature T_c has been established by introducing the hydrostatic and chemical pressure in both $\text{Sr}_3\text{Rh}_4\text{Sn}_{13}$ and $\text{Sr}_3\text{Ir}_4\text{Sn}_{13}$ [1,3,4]. These observations bear a great resemblance to those observed in iron pnictide superconducting systems such as $\text{La}(\text{O}_{1-x}\text{F}_x\text{FeAs})$, BaFe_2As_2 , and FeSe [10–13]. While the formation of the spin-density-wave (SDW) state below T^* has been unambiguously resolved in the case of iron pnictide superconductors [13–17], the scenario for the existence of the CDW state below T^* in $\text{Sr}_3\text{Rh}_4\text{Sn}_{13}$ and $\text{Sr}_3\text{Ir}_4\text{Sn}_{13}$ is still a matter of debate.

In this regard, a question which naturally arises is whether an examination of the phase transitions in $\text{Sr}_3\text{Rh}_4\text{Sn}_{13}$ and $\text{Sr}_3\text{Ir}_4\text{Sn}_{13}$ will yield results similar to those in the well-

established CDW systems. With the aim of obtaining additional insight into the thermodynamic properties near the structural phase transitions in both materials, we carried out specific-heat C_p and thermal-expansion measurements, mainly focusing on the temperature region around each T^* . It is known that specific heat and thermal expansion are useful thermodynamic probes to explore the nature of phase transition in solids. A quantitative analysis of the C_p data reveals that each spiky specific-heat peak observed in the vicinity of T^* is essentially associated with the contribution from thermal fluctuations. In addition, a large enhancement of the specific-heat jump compared to the electronic mean-field jump deduced from the analysis indicates the strong-coupling nature of the phase transitions. Furthermore, the T -dependent thermal expansivity allows us to characterize the fundamental thermodynamic properties, providing more information about the structural phase transitions observed in both compounds.

II. EXPERIMENTAL RESULTS AND DISCUSSION

Single crystals of $\text{Sr}_3\text{Rh}_4\text{Sn}_{13}$ and $\text{Sr}_3\text{Ir}_4\text{Sn}_{13}$ were grown by the tin self-flux method as described previously [1–4,6,18]. Photographs of the crystals with dimensions of several millimeters are shown in the top insets of Figs. 1(a) and 1(b). Both crystals were characterized as having a mosaic width of about 0.1° as measured on (440) and prealigned to have a (110) direction as the normal direction using our in-house x-ray facility. A further study using synchrotron x-ray scattering was carried out on the BL07 beamline at the National Synchrotron Radiation Research Center (NSRRC) located in Hsinchu, Taiwan. The crystal was glued on a closed-cycle cryostat mounted on an eight-circle diffractometer. The use of the multicircle diffractometer allows the measurements to be performed along any crystal axis in reciprocal space. In order to enhance the resolution, high-quality single-crystal LiF was used as an analyzer to analyze the scattered x rays from the

*cslue@mail.ncku.edu.tw

†ykkuo@mail.ndhu.edu.tw

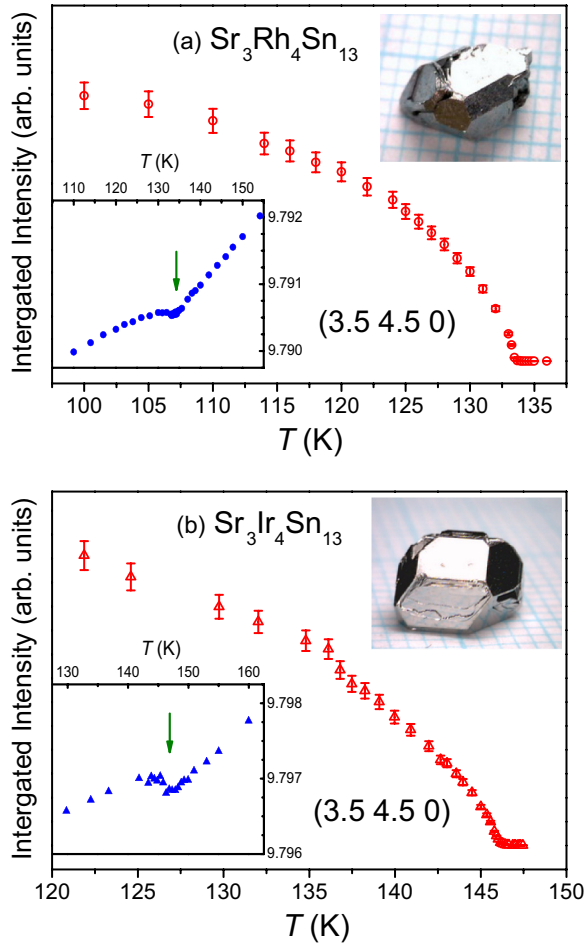


FIG. 1. Integrated intensity of the superstructure Bragg reflection at $(3.5\ 4.5\ 0)$ as a function of temperature for (a) $\text{Sr}_3\text{Rh}_4\text{Sn}_{13}$ and (b) $\text{Sr}_3\text{Ir}_4\text{Sn}_{13}$. The bottom insets show the evolution of the lattice parameter in armstrongs at around T^* , indicated by an arrow. The top insets show the representative $\text{Sr}_3\text{Rh}_4\text{Sn}_{13}$ and $\text{Sr}_3\text{Ir}_4\text{Sn}_{13}$ single crystals used in this study.

sample. The incident x rays were selected to be 14 KeV by a pair of Si crystals of (111).

We also measured a Bragg reflection of (440) as a function of temperature for each specimen. The evolutions of the lattice parameter for $\text{Sr}_3\text{Rh}_4\text{Sn}_{13}$ and $\text{Sr}_3\text{Ir}_4\text{Sn}_{13}$, extracted from the peak position of (440) , are illustrated in the bottom insets of Figs. 1(a) and 1(b). Unlike the first-order structural phase transition, which shows a discontinuous jump or drop in the lattice parameter at the phase-transition temperature, the observed T -dependent lattice parameter only exhibits a distinctive feature near the corresponding T^* . Such observations provide strong evidence of the nature of the second-order phase transition of both materials. It should be noted that the presented values below T^* are one half of the lattice parameters since the lattice parameter of the low-temperature phase has been identified as two times that of the high-temperature phase [1,4]. Upon cooling below T^* , a linear scan through the longitudinal direction reveals additional Bragg reflections associated with a structural modulation indexed by a wave vector $\mathbf{q} = (0.5\ 0.5\ 0)$. For $\text{Sr}_3\text{Rh}_4\text{Sn}_{13}$ and $\text{Sr}_3\text{Ir}_4\text{Sn}_{13}$, we recorded the temperature variations of the integrated intensity

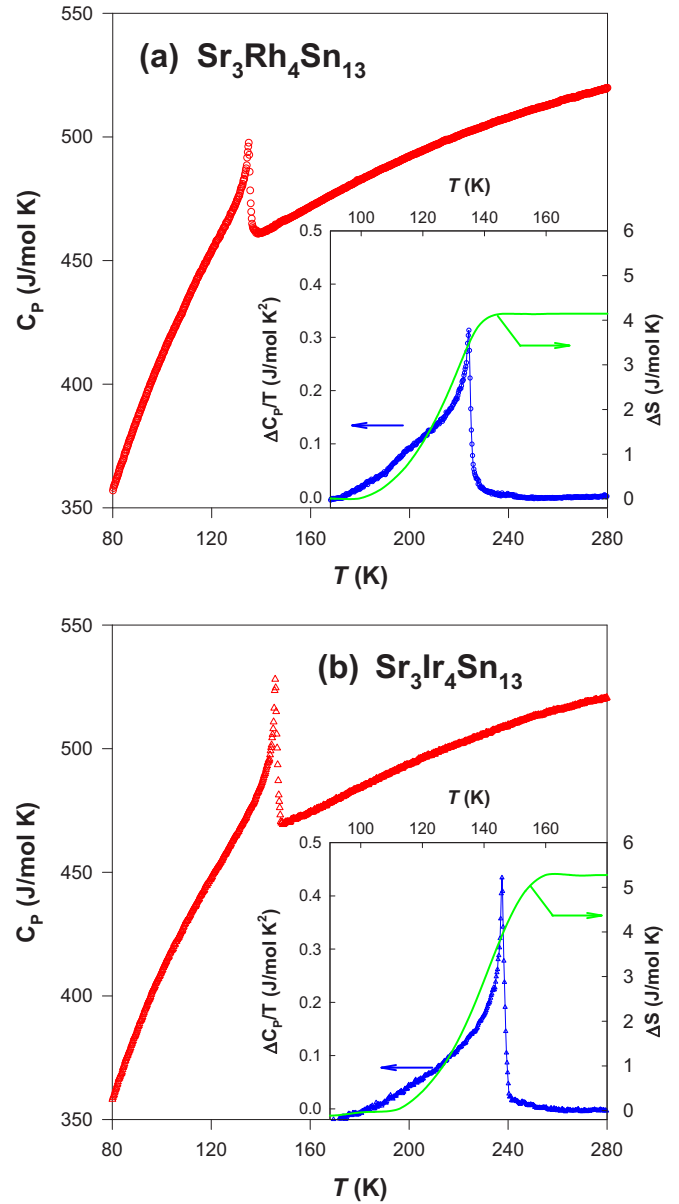


FIG. 2. Temperature dependence of specific heat for (a) $\text{Sr}_3\text{Rh}_4\text{Sn}_{13}$ and (b) $\text{Sr}_3\text{Ir}_4\text{Sn}_{13}$. The insets show a plot of $\Delta C_p/T$ vs T and the entropy change ΔS associated with the transition.

of the superstructure peak at $(3.5\ 4.5\ 0)$, with the results displayed in Figs. 1(a) and 1(b), respectively. It is apparent that the integrated intensity of each superstructure peak decreases continuously as the temperature approaches T^* , a typical characteristic of the second-order phase transition. A similar observation at $(3.5\ 3.5\ 0)$ in the isostructural compound $\text{Ca}_3\text{Ir}_4\text{Sn}_{13}$ has been reported as $T < T^* \simeq 38\ \text{K}$ [19].

Specific-heat measurements were performed with a high-resolution ac calorimeter using chopped light as a heat source. The ac technique is known as a powerful tool providing denser and smoother data in a narrow temperature range during a sharp phase transition. Further details about the experimental technique can be found elsewhere [20]. The observed temperature variations of C_p for $\text{Sr}_3\text{Rh}_4\text{Sn}_{13}$ and $\text{Sr}_3\text{Ir}_4\text{Sn}_{13}$ are shown in Figs. 2(a) and 2(b), respectively. For each material, a spiky peak with no thermal hysteresis around

TABLE I. Summary of thermodynamic quantities at T^* for $\text{Sr}_3\text{Rh}_4\text{Sn}_{13}$ and $\text{Sr}_3\text{Ir}_4\text{Sn}_{13}$ compared to the well-studied 3D CDW system of $\text{Lu}_5\text{Ir}_4\text{Si}_{10}$ with data deduced from Ref. [21].

Compound	T^* (K)	ΔC_p (J/mol K)	ΔS (R)	$\Delta C_p/C_{MF}$
$\text{Sr}_3\text{Rh}_4\text{Sn}_{13}$	135.2	42.3	0.58	2.0
$\text{Sr}_3\text{Ir}_4\text{Sn}_{13}$	146.3	66.3	0.63	3.1
$\text{Lu}_5\text{Ir}_4\text{Si}_{10}$	79.8	55.0	0.12	8.9

T^* in C_p confirms the second-order nature of this phase transition. To evaluate the specific-heat jump ΔC_p and the entropy change ΔS near the corresponding phase transition, we have estimated the lattice background from 80 to 300 K for each sample by fitting a lattice background through the data far from the transition region. The T -dependent ΔC_p can be obtained by subtracting the lattice background from the experimental data. The corresponding ΔS is, in turn, evaluated by integrating the area under $\Delta C_p/T$ versus T curves as shown in the insets of Figs. 2(a) and 2(b). The extracted values of ΔC_p at T^* and ΔS are tabulated in Table I.

The large values of $\Delta S = 0.58R$ for $\text{Sr}_3\text{Rh}_4\text{Sn}_{13}$ and $0.63R$ for $\text{Sr}_3\text{Ir}_4\text{Sn}_{13}$, where R is the gas constant, suggest a strong electron-phonon coupling in their phase transitions. This could be attributed to a contribution from the phonon softening that results in a Kohn anomaly [21]. It is worth mentioning that the excess specific heats $\Delta C_p/C_p$ of about 10% for $\text{Sr}_3\text{Rh}_4\text{Sn}_{13}$ and 14% for $\text{Sr}_3\text{Ir}_4\text{Sn}_{13}$ are comparable to those of the well-established three-dimensional (3D) CDW compounds such as $\text{Lu}_5\text{Ir}_4\text{Si}_{10}$ ($\simeq 26\%$), $\text{Lu}_5\text{Rh}_4\text{Si}_{10}$ ($\simeq 12\%$), and $\text{Er}_5\text{Ir}_4\text{Si}_{10}$ ($\simeq 18\%$) [20,22–24]. The comparison points out the strong similarity in the thermodynamic features around their phase transitions.

Since the observed phase transitions in $\text{Sr}_3\text{Rh}_4\text{Sn}_{13}$ and $\text{Sr}_3\text{Ir}_4\text{Sn}_{13}$ have been identified as a second-order transition in nature, we can thus quantitatively analyze the C_p data in the framework of the critical fluctuation model in addition to mean-field contributions within its transition region. On this basis, C_p consists of three terms, given as

$$C_p = C_L + C_{MF} + C_{FL}, \quad (1)$$

where C_L is the lattice background, C_{MF} is the mean-field term below T^* , and C_{FL} is associated with fluctuation contributions. Here, the lattice specific heat can be described by the Einstein model as

$$C_L = a_1 \left(\frac{a_2}{T} \right)^{a_3} \frac{e^{a_2/T}}{(e^{a_2/T} - 1)^2}. \quad (2)$$

The mean-field term below T^* is represented by $C_{MF} = \gamma^* T^* (1 + \beta t)$, and the fluctuation part is $C_{FL}^- = b^-/|t|^{\alpha^-}$ as $T < T^*$ and $C_{FL}^+ = b^+/|t|^{\alpha^+}$ as $T > T^*$. In order to fit the total specific heat, the fitting functions below (C^-) and above (C^+) T^* can be expressed as

$$C^- = C_L + \gamma^* T^* (1 + \beta t) + b^-/|t|^{\alpha^-}, \quad T < T^*, \quad (3)$$

$$C^+ = C_L + b^+/|t|^{\alpha^+}, \quad T > T^*. \quad (4)$$

Here $a_1, a_2, a_3, \gamma^*, \beta, b^-, b^+, \alpha^-,$ and α^+ are effective fitting parameters, where α^- and α^+ are known as critical exponents

and $t = (T - T^*)/T^*$ is the reduced temperature. Thus the specific-heat jump $C_{MF} = \gamma^* T^*$ at T^* predicted by the mean-field theory can be obtained. It is worth mentioning that the Gaussian approximation is a first-order correction to the mean-field theory to describe the critical fluctuations near T^* , where the critical exponents $\alpha^- = \alpha^+ = 0.5$ are expected with the effective 3D fluctuations.

The fitting procedures were then taken as follows: we first took $T^* = 135.2$ and 146.3 K for $\text{Sr}_3\text{Rh}_4\text{Sn}_{13}$ and $\text{Sr}_3\text{Ir}_4\text{Sn}_{13}$, respectively, and then used the experimental C_p data above and away from T^* to find the best-fitting values of $a_1, a_2,$ and a_3 for C_L . With the obtained C_L , the optimum values of γ^* and β for each material can be found by fitting the C_p curve below and near but not too close to T^* to the function of $C_L + C_{MF}$. We then determined the best-fitting values of b^-, α^- and b^+, α^+ by adjusting the functions $(C_L + C_{MF} + C_{FL})$ and $(C_L + C_{FL})$ for temperatures below and above T^* , respectively, to match the measured C_p curves. Such a nonlinear least-squares fitting process was performed iteratively by refining all fitting parameters until the best fit to the experimental data was achieved. A satisfactory agreement between the fits and measured data of $\text{Sr}_3\text{Rh}_4\text{Sn}_{13}$ and $\text{Sr}_3\text{Ir}_4\text{Sn}_{13}$ is clearly seen, as illustrated in Figs. 3(a) and 3(b), respectively.

The extracted fitting parameters reveal important information about the characteristics of the phase transitions in both $\text{Sr}_3\text{Rh}_4\text{Sn}_{13}$ and $\text{Sr}_3\text{Ir}_4\text{Sn}_{13}$. We found that $a_1, a_2,$ and a_3 are nearly identical, which is reasonable as both materials share the same crystal structure and, in turn, have a similar lattice background. The critical exponents $\alpha^- = 0.5$ and $\alpha^+ = 0.45$ were extracted from the best fit for $\text{Sr}_3\text{Rh}_4\text{Sn}_{13}$, as expected from the extended mean-field expectation of 3D fluctuations. However, larger critical exponents of $\alpha^- = 0.75$ and $\alpha^+ = 0.65$ were obtained for $\text{Sr}_3\text{Ir}_4\text{Sn}_{13}$. A higher power of divergence in C_p near T^* reflects the fact that the transition width in ΔC_p of $\text{Sr}_3\text{Ir}_4\text{Sn}_{13}$ is narrower than that of $\text{Sr}_3\text{Rh}_4\text{Sn}_{13}$, suggesting that $\text{Sr}_3\text{Ir}_4\text{Sn}_{13}$ has a shorter coherence length responsible for the phase transition [25].

Another important quantity $\gamma^* = 0.16$ and 0.14 J/mol K² was extracted from the fits for $\text{Sr}_3\text{Rh}_4\text{Sn}_{13}$ and $\text{Sr}_3\text{Ir}_4\text{Sn}_{13}$, respectively. This leads to the electronic mean-field specific-heat jumps $C_{MF} = \gamma^* T^* = 21.6$ and 20.5 J/mol K for the corresponding compounds. It is noted that the estimated mean-field contribution accounts for about one half ($\text{Sr}_3\text{Rh}_4\text{Sn}_{13}$) and one third ($\text{Sr}_3\text{Ir}_4\text{Sn}_{13}$) of the total specific-heat jump ΔC_p (see Table I), indicating that critical fluctuations play an important role at the phase transition for these compounds. Taking the experimental values of the electronic specific-heat coefficient of 34.8 mJ/mol K² for $\text{Sr}_3\text{Rh}_4\text{Sn}_{13}$ and of about 40 mJ/mol K² for $\text{Sr}_3\text{Ir}_4\text{Sn}_{13}$ [4,7,18], we obtained the ratios of $\gamma^*/\gamma = 4.6$ and 3.5 for $\text{Sr}_3\text{Rh}_4\text{Sn}_{13}$ and $\text{Sr}_3\text{Ir}_4\text{Sn}_{13}$, respectively. Both values are much larger than the BCS value of 1.43 within the weak-coupling limit. Such an enhancement in ΔC_p from its mean-field value has been reported in the 3D CDW system of $\text{Lu}_5\text{Ir}_4\text{Si}_{10}$ ($\gamma^*/\gamma \simeq 8.4$), which has been attributed to the strong-coupling nature of the observed phase transition [20]. The scenario for the strong-coupling phase transition in $\text{Sr}_3\text{Ir}_4\text{Sn}_{13}$ has been proposed by Fang and coworkers, based on their observation of a high ratio of energy gap relative to T^* revealed by the optical spectroscopy study [7].

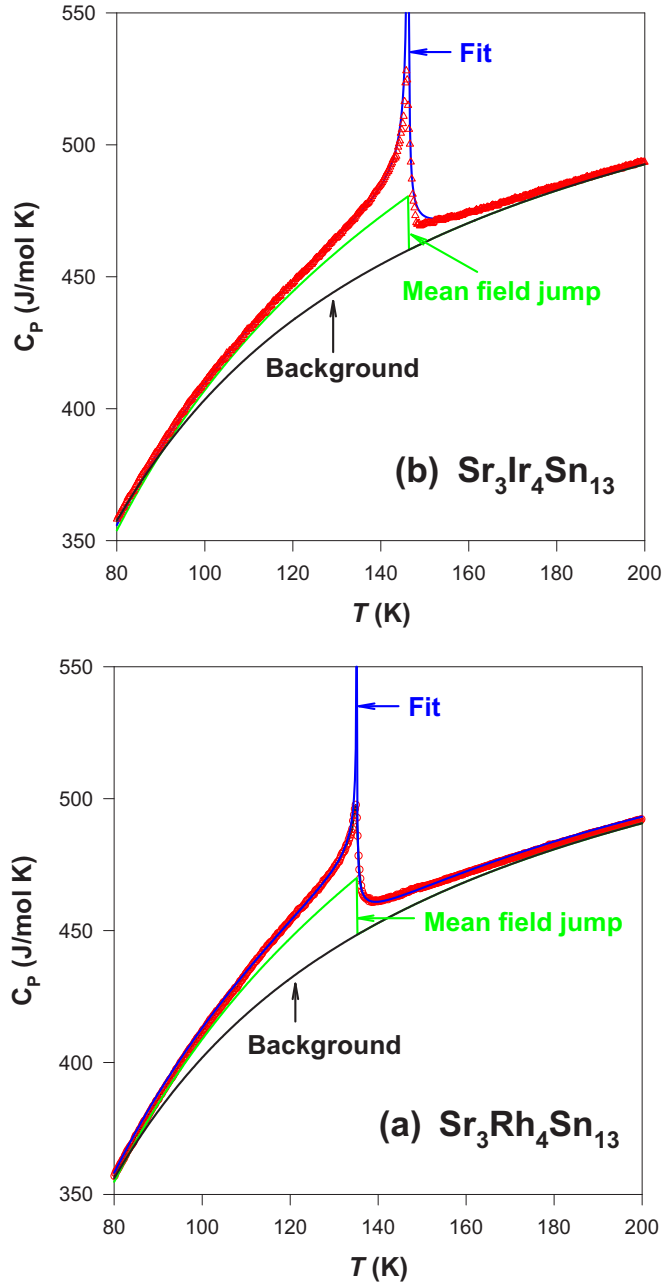


FIG. 3. The agreement between the measured data and the fit (solid blue lines) in the vicinity of transitions for (a) $\text{Sr}_3\text{Rh}_4\text{Sn}_{13}$ and (b) $\text{Sr}_3\text{Ir}_4\text{Sn}_{13}$. The theoretical fit employs a model including critical fluctuations and mean-field contributions.

The linear thermal expansivity $\Delta L/L$ was measured using a capacitance dilatometer which was calibrated against standard copper and aluminum specimens. The relative sensitivity of our dilatometer is about 10^{-10} for the sample with similar dimensions. For each specimen, a close-up plot of $\Delta L/L$ in the vicinity of T^* is given in the insets of Figs. 4(a) and 4(b), respectively. It is noticeable that the features of $\Delta L/L$ near the phase transitions are very similar to those of the lattice parameter shown in the insets of Figs. 1(a) and 1(b). The T -dependent coefficients of the linear thermal expansion α_L for $\text{Sr}_3\text{Rh}_4\text{Sn}_{13}$ and $\text{Sr}_3\text{Ir}_4\text{Sn}_{13}$ are illustrated in Figs. 4(a) and 4(b),

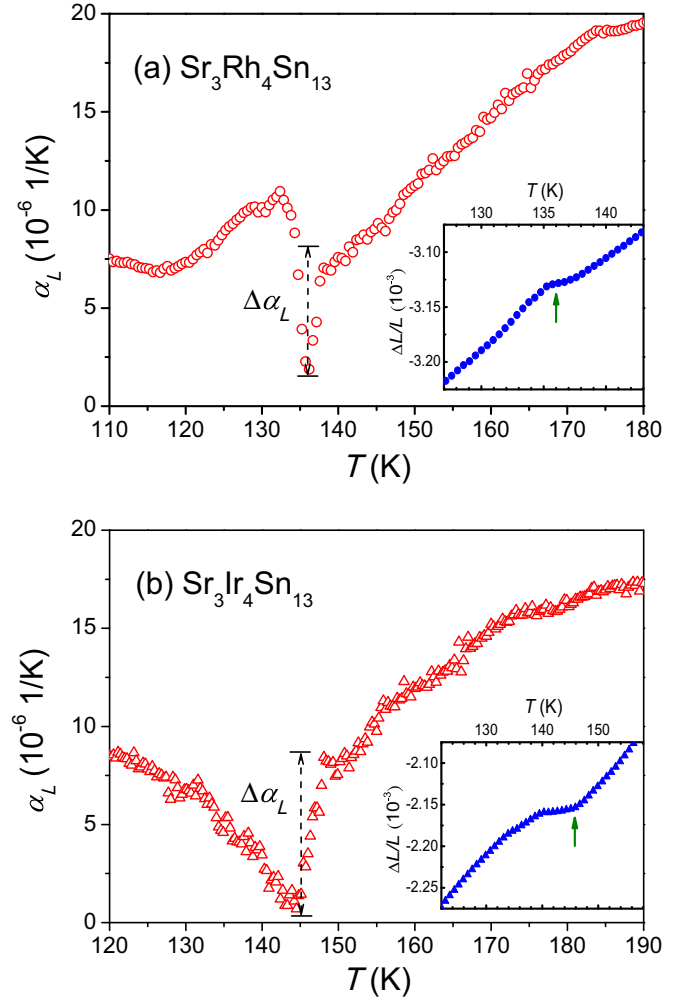


FIG. 4. Temperature dependence of the coefficient of linear thermal expansion α_L of (a) $\text{Sr}_3\text{Rh}_4\text{Sn}_{13}$ and (b) $\text{Sr}_3\text{Ir}_4\text{Sn}_{13}$. The insets show the relative length change $\Delta L/L$ in the vicinity of T^* , indicated by an arrow for each studied compound.

respectively. For each material, a negative dip in α_L appears at the onset of the phase transition. In principle, the observation of a pronounced change in α_L during the phase transition can be attributed to the presence of soft phonons, which in turn leads to a large pressure effect on the transition temperature. As a matter of fact, rather high suppression of T^* under hydrostatic pressure for both $\text{Sr}_3\text{Rh}_4\text{Sn}_{13}$ ($dT^*/dP \simeq -2.0$ K/kbar) and $\text{Sr}_3\text{Ir}_4\text{Sn}_{13}$ ($dT^*/dP \simeq -2.1$ K/kbar) has been reported [1,4]. The scenario for the structural phase transitions associated with the soft phonon modes in $\text{Sr}_3\text{Rh}_4\text{Sn}_{13}$ and $\text{Sr}_3\text{Ir}_4\text{Sn}_{13}$ has been further established by Tompsett *et al.* based on their calculations for the corresponding phonon dispersion relations [1,5].

According to the Ehrenfest relation for a second-order phase transition [26], the pressure-dependent transition temperature dT^*/dP can be derived from the thermal-expansion temperature jump $\Delta\alpha_L$ together with the specific-heat jump ΔC_p as

$$\frac{dT^*}{dP} = 3VT^* \frac{\Delta\alpha_L}{\Delta C_p}. \quad (5)$$

As revealed from Figs. 4(a) and 4(b), we determined $\Delta\alpha_L \simeq -6.9 \times 10^{-6} \text{ K}^{-1}$ for $\text{Sr}_3\text{Rh}_4\text{Sn}_{13}$ and $-8.4 \times 10^{-6} \text{ K}^{-1}$ for $\text{Sr}_3\text{Ir}_4\text{Sn}_{13}$, respectively. Substituting the molar volume $V = 2.83 \times 10^{-4} \text{ m}^3/\text{mol}$ and the corresponding values of T^* and ΔC_p in the above relation, it yields $dT^*/dP = -1.9 \text{ K/kbar}$ for $\text{Sr}_3\text{Rh}_4\text{Sn}_{13}$ and -1.6 K/kbar for $\text{Sr}_3\text{Ir}_4\text{Sn}_{13}$. It is found that both results are in good agreement with the experimental values [1,4], indicating that the thermodynamic quantities for the phase transitions of $\text{Sr}_3\text{Rh}_4\text{Sn}_{13}$ and $\text{Sr}_3\text{Ir}_4\text{Sn}_{13}$ obey the classical thermodynamic relations.

Another thermodynamic discontinuity which occurs during a second-order phase transition is the change in the isothermal compressibility $\Delta\kappa_T$, given by another Ehrenfest equation as

$$\Delta\kappa_T = 3\Delta\alpha_L \left(\frac{dT^*}{dP} \right). \quad (6)$$

We therefore extracted $\Delta\kappa_T \simeq -3.9 \times 10^{-9}$ per bar for $\text{Sr}_3\text{Rh}_4\text{Sn}_{13}$ and $\simeq -4 \times 10^{-9}$ per bar for $\text{Sr}_3\text{Ir}_4\text{Sn}_{13}$ undergoing the structural phase transitions. For crystalline solids, it is more instructive to convert the isothermal compressibility into the bulk modulus B . We thus estimated the change in the bulk modulus $\Delta B \simeq -B^2\Delta\kappa_T \simeq 4 \text{ GPa}$ by taking the same value of $B = 96 \text{ GPa}$ for $\text{Ca}_3\text{Rh}_4\text{Sn}_{13}$ at an ambient pressure [27]. The increasing bulk modulus across T^* implies that $\text{Sr}_3\text{Rh}_4\text{Sn}_{13}$ and $\text{Sr}_3\text{Ir}_4\text{Sn}_{13}$ become stiffer as they transform to the low-temperature crystal structure. To our knowledge, no measurements of compressibility and bulk modulus have been carried out in the vicinity of the phase transitions on $\text{Sr}_3\text{Rh}_4\text{Sn}_{13}$ and $\text{Sr}_3\text{Ir}_4\text{Sn}_{13}$. Therefore the application of these thermodynamic relations allows us to estimate the variations in the compressibility and bulk modulus at the phase transitions for both compounds.

It is worth remarking that in addition to $\text{Sr}_3\text{Rh}_4\text{Sn}_{13}$ and $\text{Sr}_3\text{Ir}_4\text{Sn}_{13}$, there are several isostructural analogs such as $\text{Eu}_3\text{Ir}_4\text{Sn}_{13}$, $\text{Ce}_3\text{Co}_4\text{Sn}_{13}$, and $\text{La}_3\text{Co}_4\text{Sn}_{13}$ that exhibit exotic

phase transitions [28–33]. However, the measurements of the specific heat in these materials indicated relatively weak changes in ΔC_p at the corresponding T^* [28,30,33]. In this respect, the unique characteristics of the phase transitions in the present cases of $\text{Sr}_3\text{Rh}_4\text{Sn}_{13}$ and $\text{Sr}_3\text{Ir}_4\text{Sn}_{13}$ are quite different from those in the aforementioned compounds. Instead, their thermodynamic properties revealed from the current investigation bear a striking resemblance to those found in the 3D CDW systems $R_3\text{Ir}_4\text{Si}_{10}$ in many respects [20,23,24].

III. SUMMARY

We have successfully grown single crystals of $\text{Sr}_3\text{Rh}_4\text{Sn}_{13}$ and $\text{Sr}_3\text{Ir}_4\text{Sn}_{13}$ and conducted detailed characterizations by specific-heat and thermal-expansivity measurements. In particular, the quantitative analysis of the C_p data in the framework of the critical fluctuation model in addition to mean-field contributions provides important thermodynamic information about their structural phase transitions. Relatively large critical exponents were obtained for $\text{Sr}_3\text{Ir}_4\text{Sn}_{13}$, suggesting a shorter coherence length is responsible for the phase transition. An enhancement in the electronic specific-heat jump from its mean-field value has been quantitatively identified for both compounds, revealing the strong-coupling nature of the observed phase transitions. Furthermore, a negative pressure dependence of the transition temperature and a positive change of the bulk modulus across the corresponding phase transition have been established through the present investigation.

ACKNOWLEDGMENTS

This work was supported by the Ministry of Science and Technology of Taiwan under Grants No. MOST-103-2112-M-006-014-MY3 (C.S.L.) and No. MOST-103-2112-M-259-008-MY3 (Y.K.K.).

-
- [1] S. K. Goh, D. A. Tompsett, P. J. Saines, H. C. Chang, T. Matsumoto, M. Imai, K. Yoshimura, and F. M. Grosche, *Phys. Rev. Lett.* **114**, 097002 (2015).
- [2] C. N. Kuo, C. W. Tseng, C. M. Wang, C. Y. Wang, Y. R. Chen, L. M. Wang, C. F. Lin, K. K. Wu, Y. K. Kuo, and C. S. Lue, *Phys. Rev. B* **91**, 165141 (2015).
- [3] W. C. Yu, Y. W. Cheung, P. J. Saines, M. Imai, T. Matsumoto, C. Michioka, K. Yoshimura, and S. K. Goh, *Phys. Rev. Lett.* **115**, 207003 (2015).
- [4] L. E. Klitberg, S. K. Goh, P. L. Alireza, P. J. Saines, D. A. Tompsett, P. W. Logg, J. Yang, B. Chen, K. Yoshimura, and F. M. Grosche, *Phys. Rev. Lett.* **109**, 237008 (2012).
- [5] D. A. Tompsett, *Phys. Rev. B* **89**, 075117 (2014).
- [6] C. N. Kuo, H. F. Liu, C. S. Lue, L. M. Wang, C. C. Chen, and Y. K. Kuo, *Phys. Rev. B* **89**, 094520 (2014).
- [7] A. F. Fang, X. B. Wang, P. Zheng, and N. L. Wang, *Phys. Rev. B* **90**, 035115 (2014).
- [8] P. K. Biswas, A. Amato, R. Khasanov, H. Luetkens, Kefeng Wang, C. Petrovic, R. M. Cook, M. R. Lees, and E. Morenzoni, *Phys. Rev. B* **90**, 144505 (2014).
- [9] L. M. Wang, C.-Y. Wang, G.-M. Chen, C. N. Kuo, and C. S. Lue, *New J. Phys.* **17**, 033005 (2015).
- [10] Y. Kamihara, T. Watanabe, M. Hirano, and H. Hosono, *J. Am. Chem. Soc.* **130**, 3296 (2008).
- [11] M. Rotter, M. Tegel, and D. Johrendt, *Phys. Rev. Lett.* **101**, 107006 (2008).
- [12] J. Paglione and R. L. Greene, *Nat. Phys.* **6**, 645 (2010).
- [13] T. Imai, K. Ahilan, F. L. Ning, T. M. McQueen, and R. J. Cava, *Phys. Rev. Lett.* **102**, 177005 (2009).
- [14] C. de la Cruz, Q. Huang, J. W. Lynn, J. Li, W. Ratcliff, II, J. L. Zarestky, H. A. Mook, G. F. Chen, J. L. Luo, N. L. Wang, and P. Dai, *Nature (London)* **453**, 899 (2008).
- [15] J. Dong, H. J. Zhang, G. Xu, Z. Li, G. Li, W. Z. Hu, D. Wu, G. F. Chen, X. Dai, J. L. Luo, Z. Fang, and N. L. Wang, *Europhys. Lett.* **83**, 27006 (2008).
- [16] M. Rotter, M. Tegel, D. Johrendt, I. Schellenberg, W. Hermes, and R. Pottgen, *Phys. Rev. B* **78**, 020503 (2008).
- [17] W. Bao, Y. Qiu, Q. Huang, M. A. Green, P. Zajdel, M. R. Fitzsimmons, M. Zhernenkov, S. Chang, M. Fang, B. Qian, E. K. Vehstedt, J. Yang, H. M. Pham, L. Spinu, and Z. Q. Mao, *Phys. Rev. Lett.* **102**, 247001 (2009).

- [18] N. Kase, H. Hayamizu, and J. Akimitsu, *Phys. Rev. B* **83**, 184509 (2011).
- [19] D. G. Mazzone, S. Gerber, J. L. Gavilano, R. Sibille, M. Medarde, B. Delley, M. Ramakrishnan, M. Neugebauer, L. P. Regnault, D. Chernyshov, A. Piovano, T. M. Fernandez-Diaz, L. Keller, A. Cervellino, E. Pomjakushina, K. Conder, and M. Kenzelmann, *Phys. Rev. B* **92**, 024101 (2015).
- [20] Y.-K. Kuo, C. S. Lue, F. H. Hsu, H. H. Li, and H. D. Yang, *Phys. Rev. B* **64**, 125124 (2001).
- [21] D. E. Moncton, J. D. Axe, and F. J. DiSalvo, *Phys. Rev. Lett.* **34**, 734 (1975).
- [22] C. S. Lue, Y.-K. Kuo, F. H. Hsu, H. H. Li, H. D. Yang, P. S. Fodor, and L. E. Wenger, *Phys. Rev. B* **66**, 033101 (2002).
- [23] F. Galli, S. Ramakrishnan, T. Taniguchi, G. J. Nieuwenhuys, J. A. Mydosh, S. Geupel, J. Ludecke, and S. van Smaalen, *Phys. Rev. Lett.* **85**, 158 (2000).
- [24] Y. K. Kuo, F. H. Hsu, H. H. Li, H. L. Huang, C. W. Huang, C. S. Lue, and H. D. Yang, *Phys. Rev. B* **67**, 195101 (2003).
- [25] W. L. McMillan, *Phys. Rev. B* **16**, 643 (1977).
- [26] P. Ehrenfest, Commum. Kamerlingh Onnes Lab., Leiden, **20** Suppl. 75b, 8 (1933).
- [27] A. Haas, D. Wichert, G. Bruls, B. Luthi, G. Balakrishnan, and D. McK. Paul, *J. Low Temp. Phys.* **114**, 285 (1999).
- [28] L. Mendonca Ferreira, E. M. Bittar, M. A. Pires, R. R. Urbano, O. Agüero, I. Torriani, C. Rettori, P. G. Pagliuso, A. Malachias, E. Granado, A. Caytuero, and E. Baggio-Saitovich, *Phys. B (Amsterdam, Neth.)* **384**, 332 (2006).
- [29] J. R. L. Mardegan, N. Aliouane, L. N. Coelho, O. Agüero, E. M. Bittar, J. C. Lang, P. G. Pagliuso, I. L. Torriani, and C. Giles, *IEEE Trans. Magn.* **49**, 4652 (2013).
- [30] C. S. Lue, H. F. Liu, S. L. Hsu, M. W. Chu, H. Y. Liao, and Y. K. Kuo, *Phys. Rev. B* **85**, 205120 (2012).
- [31] A. Slebarski, B. D. White, M. Fijalkowski, J. Goraus, J. J. Hamlin, and M. B. Maple, *Phys. Rev. B* **86**, 205113 (2012).
- [32] J. R. Collave, H. A. Borges, S. M. Ramos, E. N. Hering, M. B. Fontes, E. Baggio-Saitovitch, L. Mendonca-Ferreira, E. M. Bittar, and P. G. Pagliuso, *J. Appl. Phys.* **117**, 17E307 (2015).
- [33] H. F. Liu, C. N. Kuo, C. S. Lue, K.-Z. Syu, and Y. K. Kuo, *Phys. Rev. B* **88**, 115113 (2013).